Sato et al., Aerosol and Air Quality Research, Vol. 7, No. 3, pp. 278-303, 2007

Molecular Dynamics Study of Nanoparticle Collision with a Surface – Implication to Nanoparticle Filtration

Shintaro Sato[1*], Da-Ren Chen[2], David Y. H. Pui[1]**

[1]*Particle Technology Laboratory, Mechanical Engineering Department, University of Minnesota, 111 Church St. SE, Minneapolis, MN 55455, USA.*

[2]*Department of Mechanical Engineering, Join Program in Environmental Engineering Science, Washington University in St. Louis, St. Louis, MO 63141, USA.*

Abstract

Collision dynamics of nanoparticles with a surface was studied by classical molecular dynamics simulations. Silver, nickel and silica were selected as the particle materials, and silver as the surface material. Particle sizes ranged approximately from 0.5 to 2 nm. The results indicate that particles with thermal energy at room temperature do not bounce off a surface, even when a very weak interaction potential between the particles and the surface is assumed. The loss mechanisms of the center-of-mass energy of nanoparticles colliding with a surface were also investigated. The findings indicate that energy losses to the surface and the rotational degree of freedom are important. The loss to the surface is significant when a harder particle hits a softer surface. This is because the center-of-mass energy is mainly transferred to the surface as elastic energy, and the energy is not effectively transferred back to the particle. Non-spherical silica particles were found to lose more energy than the other types of particles. This phenomenon is due to a large energy transfer to the rotational degree of the freedom upon collision.

Keywords: Molecular dynamics; Nanoparticle collision; Nanoparticle filtration.

[*] Current address: Fujitsu Laboratories Ltd. 10-1 Morinosato-Wakamiya, Atsugi, Kanagawa 243-0197, Japan

[**] Corresponding author. Tel: 314-935-7924; Fax: 314-935-5464

E-*mail address*: chen@me.wustl.edu

INTRODUCTION

The collision of nanoparticles (particles smaller than approximately 50 nm in diameter) with surfaces is relevant to many practical applications. Examples are the nanoparticle collection after they are synthesized in chemical reactors or emitted from mobile/stationary combustion sources, micro-contamination control in semiconductor processes, and worker protection in industrial hygiene. Filtration is a typical technique for particle control and removal. According to the traditional single-fiber theory the filtration of nanoparticles is an easy task due to the high diffusion coefficient of nanoparticles. On the other hand, it is a fact that filters cannot remove air molecules. In order to bridge the gap between particle and molecule sciences, Wang and Kasper (1991) argued that nanoparticles smaller than certain sizes might penetrate filters by bouncing off the filter surfaces due to their thermal velocity (thermal rebound). It could represent a serious problem because more evidence indicates that nanoparticles have serious adverse health effects (Donaldson, *et al.*, 1998). The main motivation of this study is to assess the possibility of nanoparticle penetration through filter media.

The stickiness of nanoparticles on a filter medium surface depends on the loss of center-of-mass energy of the incident particles due to the collision. The energy loss mechanisms include the transfer of incident energy to the rotation, vibration, and deformation of the particle, and energy transfer to the impact surface. The significance of each mechanism is thought to depend on parameters, such as the incident energy, particle-surface interaction, elastic properties of particle and surface, and particle characteristics. Such energy loss mechanisms are, however, not yet well understood in the incident velocity ranges of interest (up to a few hundred meters per second).

The impact of micron-sized particles with a surface for a relatively low incident velocity (typically less than 100 m/s) has been studied for years. Several macroscopic models have been proposed to explain energy loss mechanisms upon the collision. Many studies have attributed the main energy loss to the plastic deformation of a particle and/or a surface (Bitter, 1963; Rogers and Reed, 1984; Reed, 1989; Wall *et al*., 1989, 1990; Tsai *et al*., 1990; Xu and Willeke, 1993; Andres, 1995). Tsai *et al*. (1990) also included the energy loss due to the plastic deformation of surface asperities and showed that this energy loss can be significant. On the other hand, Brach and Dunn (1995) and Li *et al*. (1999) argued that the strain rate due to such a collision is too high for the plastic deformation and suggested a completely different model based on the model Hunt and Crossley (1975). Their model assumes that energy is mainly dissipated in the heat forms during the collision.

In all the models described above fitting parameters were usually included and determined by the comparison with experiments. The ratio of the rebound particle velocity to the initial velocity was the main quantity measured in experiments (for instance, Dahneke, 1972, 1973, 1975; Wall

et al., 1990; Dunn *et al*., 1995; Li *et al*., 1999). A typical behavior of the ratio as a function of the incident velocity is that after the incident velocity exceeds the critical value for rebound the ratio increases rapidly with the increase of the initial velocity and then levels off. Particularly interesting is that this behavior can be explained by two completely different models: the model by Brach and Dunn (1995) and, say, the one by Wall *et al*. (1990). This seems partly because the quality of existing experimental data is not good enough to determine the main energy loss mechanism. On the other hand, one can also argue that any of the existing models are not comprehensive.

For nanoparticle filtration or bounce, several experimental studies have been reported. Otani *et al*. (1994) measured the particle penetration through a wire screen and a circular tube using silver particles with a size down to 1 nm. They observed that the penetration of particles of 2 nm or smaller through the tube was larger than that predicted by Gormley and Kennedy (1949), while the penetration through the wire screen agreed well with the prediction by Cheng and Yeh (1980). They attributed the discrepancy to the thermal bounce of particles from the tube's inner surface. Alonso *et al*. (1997) also performed a similar experiment using particles as small as 2 nm and ions (1.36 nm). Their results, however, agreed well with the theoretical prediction given by Gormley and Kennedy (1949) and Cheng and Yeh (1980). They argued that the seemingly higher penetration observed by Otani *et al*. (1994) was probably caused by the unreliable sizing of test particles.

As just described, particle-surface collision dynamics is not yet well understood for a wide range of particle sizes. In this study, the collision dynamics of nanoparticles (0.5-2 nm) with a surface was investigated using the classical molecular dynamics simulation. The incident velocity of particles was in the range of 10-1000 m/s. The microscopic approach was employed because macroscopic approaches may not be appropriate when phenomena occurring in the nanometer scale are described. There are two primary objectives in this study. The first one is to explore the possibility of the thermal rebound when nanoparticles are impacted on a surface. The second is to study the main energy loss mechanisms of nanoparticles during the collision. Detailed information obtained by the simulation facilitates understanding the collision dynamics of nanoparticles and exploring the possibility of particle thermal rebound.

MODELS FOR THERMAL REBOUND BY WANG AND KASPER (1991)

As mentioned in the previous section, many experimental studies show that there is a critical velocity for particle bounce, below which all particles stick to a surface. Many models have been proposed in order to predict the critical velocity. Wang and Kasper (1991) derived the following equation:

$$V_{cr} = \left[\frac{2E_{ad}}{m_p e^2} \right]^{1/2} \quad (1)$$

where V_{cr} is the critical velocity, E_{ad} the adhesion energy of a particle with a surface, m_p the particle mass, and e the coefficient of restitution. The coefficient of restitution was defined as:

$$e^2 = 1 - \frac{L}{KE_{cm,i}} \quad (2)$$

where $KE_{cm,i}$ is the initial center-of-mass energy of the particle, and L the energy loss in the impact.

For the adhesion energy, two different types were used. One is the Bradley-Hamaker (B-H) adhesion energy, which considers the van der Waals energy between the particle and the surface, and is proportional to the particle diameter, d_p. If this adhesion energy is assumed, the critical velocity will become inversely proportional to the particle diameter for a spherical particle. The other type of adhesion energy is based on the JKR theory (Johnson *et al.*, 1971), which considers deformation of the particle. According to the theory, the adhesion energy is proportional to $d_p^{4/3}$. Therefore, substituting the adhesion energy into Eq. 1 leads to the critical velocity proportional to $d_p^{-5/6}$.

On the other hand, the mean thermal particle velocity is proportional to the square root of the particle mass, namely, proportional to $d_p^{-1.5}$ for spherical particles. The mean thermal velocity increases more rapidly with decreasing diameter than the critical velocity above. Wang and Kasper (1991) thus argued that it is possible for the thermal velocity to exceed the critical velocity in the nanometer size range. This situation is illustrated in Fig. 1.

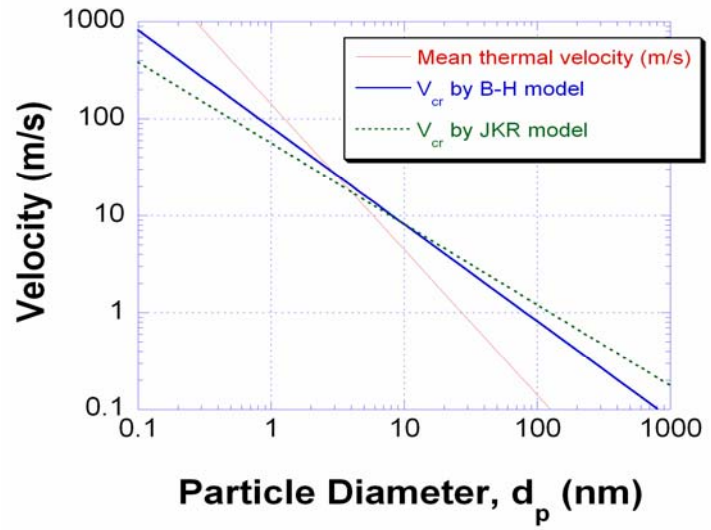

Fig. 1. Illustration of thermal rebound. The thermal velocity increases more rapidly than the critical velocity as the particle diameter decreases. The critical velocities using both the B-H model and the JKR model are shown (from Wang and Kasper, 1991).

MOLECULAR DYNAMICS SIMULATION

General description

In this study, the classical molecular dynamics (MD) simulation was used to study nanoparticle-surface collision dynamics. A typical particle-surface system is shown in Fig. 2 (a). It is not our intension, however, to study the collision dynamics for a particular particle-surface combination. Instead, the purpose is to gain a general knowledge of the nanoparticle-surface collision. In order to achieve this goal, a hypothetical interaction potential between a particle atom and a surface atom was employed. This choice will be explained later in detail.

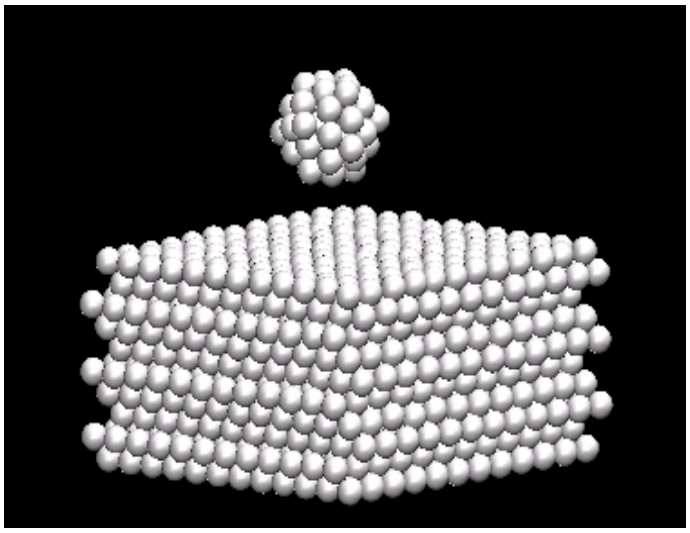

Fig. 2(a). An Ag55 particle (consisting of 55 silver atoms) and a silver surface (1440 atoms) used for the molecular dynamics simulations.

In the MD simulation, the following quantities as a function of time were extracted from the trajectories of atoms: (1) the particle trajectory; (2) the kinetic energy of nanoparticle and surface (including translational, rotational, and random motion energy); (3) the potential energy of the particle and surface; (4) the potential energy between the particle and surface. These quantities were investigated in this study as functions of the particle incident velocity, particle size, interaction potential between particle and surface atoms, particle and surface materials, and the system temperature. Special attention was paid to identify the favorable conditions for particle recoiling from the surface. Furthermore, the following assumptions were made in the simulation: (1) the impact occurs at a right angle relative to the surface; (2) the surface and particle are electrically neutral before and after the impact; and (3) the surface is smooth and free of contamination before the impact.

Particle and surface materials, and interatomic potentials

Silver material was selected as the primary particle and surface materials. This choice is partly because silver particles have normally been included in experimental studies on nanoparticle filtration, and partly because the interatomic potential for silver is well-established (Cleri and Rosato, 1993). The potential form was originally derived using quantum mechanics (e.g., Gupta, 1981), and parameters included in the potential were determined by experiments (Cleri and Rosato, 1993). The potential, called a tight-binding (TB) potential, is expressed as:

$$V_i = -\left[\sum_j \xi^2 \exp\left(-2q\left(\frac{r_{ij}}{r_0}-1\right)\right)\right]^{1/2} + \sum_j A_t \exp\left(-p\left(\frac{r_{ij}}{r_0}-1\right)\right) \quad (3)$$

The equation indicates the potential energy of an atom i by the surrounding atom j. In the equation, r_{ij} is the distance between atoms i and j, and r_0 is the first-neighbor's distance in a lattice of a metal. The parameters, ξ, q, A_t, and p are different for different transition or noble metals. The values for silver and nickel are given in Table 1. The forces exerted on atoms are obtained by taking the derivative of Eq. (3). The tight-binding potential is non-linear in nature. As proposed by Cleri and Rosato (1993), surrounding atoms up to the 5th neighbors were considered in the potential calculations.

The same tight binding potential could be used between a particle atom and a surface atom. However, for the reason described above, a hypothetical Lennard-Jones (LJ) type potential was used instead:

$$V_{LJ}(r_{ij}) = 4\varepsilon\left\{\left(\frac{\sigma}{r_{ij}}\right)^{12} - \left(\frac{\sigma}{r_{ij}}\right)^{6}\right\} \quad (4)$$

where ε is the energy parameter, σ the length parameter, and r_{ij} the distance between atoms i and j. The potential has a minimum of ε at $r_{ij} = 2^{1/6}\tilde{\sigma}$ The potential energy of an atom i is obtained by summing up $V_{LJ}(r_{ij})$ over surrounding atoms, j. The choice of this potential made it possible to study the dependence of collision dynamics on the strength of the interaction force between the particle and surface.

Table 1. Parameters for the tight binding potential.

	A_t (eV)	ξ (eV)	p	Q
Ni	0.0376	1.070	16.999	1.189
Ag	0.1208	1.178	10.928	3.139

To reduce the simulation time, it is a common practice to truncate the LJ potential at a distance of 2.5σ. However, the truncated LJ potential and force will have a discontinuity at 2.5σ, causing

numerical instabilities. In order to overcome this difficulty, the following shifted-force L-J potential (Allen and Tildesley, 1987) was used:

$$V_{LJ}^{SF}(r_{ij}) = V_{LJ}(r_{ij}) - V_{LJ}(r_{ij} = r_c) + \left(\frac{dV(r_{ij})}{dr_{ij}}\right)_{r_{ij}=r_c} (r_{ij} - r_c) \qquad (\text{for } r_{ij} < r_c)$$

$$V_{LJ}^{SF}(r_{ij}) = 0 \qquad (\text{for } r_{ij} > r_c) \qquad (5)$$

where $V_{LJ}(r_{ij})$ is the LJ potential defined in Eq. (4), and r_c the cut (truncated) distance ($r_c=2.5\sigma$).

In addition to silver, nickel and silica were used as particle materials in our study. For nickel, the TB potential with parameters shown in Table 1 was used. An empirical interatomic potential developed by Tsuneyuki *et al.* (1988) and Guissani and Guillot (1996) was used for silica. Between a nickel (or silica) particle atom and a silver surface atom, the hypothetical potential given by Eq. (5) was again used.

Parameters studied in the simulation

The ranges of parameters involved in the simulation and the particle/surface materials are summarized in Table 2. As for the surface direction, the Ag(111) surface was employed. For reference, an energy parameter of 0.02 eV is about the same as the one between Xenon atoms, and the parameter of 0.125 eV is of the same order as that between metal atoms (Blömer and Beylich, 1999). The length parameters, σ, in the LJ potential for each particle-atom/surface-atom combination are given in Table 3. For the silver/silver and nickel/silver combinations, the σ's were determined so that the potential has a minimum at the average of the nearest neighbor distances of the particle and surface materials in a bulk phase. For the oxygen/silver and silicon/silver combinations, the σ's were obtained from the van der Waals radii proposed by Huheey *et al.* (1993).

The silver and nickel particles used have an icosahedral structure, which is one of the stable structures of these particles in the size range studied. The shape of a silica particle was obtained by cooling the particle rapidly from its liquid phase. It is non-spherical, as shown in Fig. 2 (b).

Table 2. Ranges of simulation parameters, and materials for a particle and a surface.

Particle material	Silver, Nickel, Silica
Surface material	Silver
Number of atoms in a particle (Approximate size)	Silver: 13, 55, 309 (0.5, 1, 2 nm); Nickel: 13, 55, 309 (0.45, 0.9, 1.8 nm); Silica: 54 (1 nm)
Particle incident velocity	10 - 1000 m/s
Energy parameter (ε) for the particle-surface interaction	0.008, 0.02, 0.05, 0.125 eV
Temperature	298, 500 K

Table 3. Length parameters, σ, for the Lennard-Jones potential.

Particle-atom/Surface-atom	Length Parameter, σ (nm)
Silver/Silver	0.257
Nickel/Silver	0.240
Oxygen/Silver	0.285
Silicon/Silver	0.339

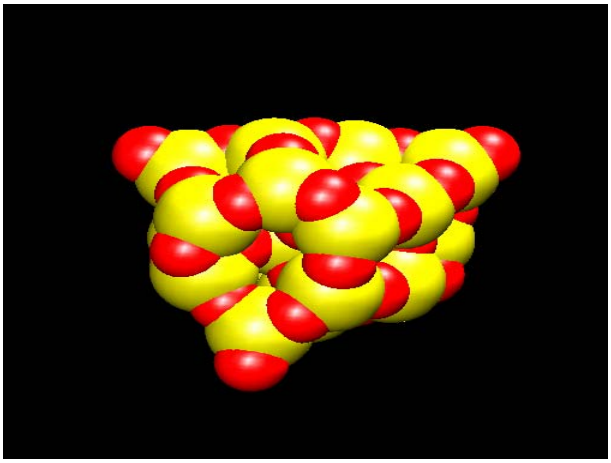

Fig. 2(b) A silica particle consisting of 36 oxygen atoms and 18 silicon atoms (Silica54). The smaller spheres show oxygen atoms.

Boundary conditions for surface domain

The surface domain for the simulation was composed of ten or more atomic layers, each of them containing a few hundred atoms. The numbers of layers and atoms in each layer depended on particle size. Periodic boundary conditions were used in the directions parallel to the surface. In the perpendicular direction, three bottom layers were fixed at the equilibrium position of the bulk material and served as the cell boundary. The sizes of simulated surfaces were chosen so that its further increase would not change the simulation results. The size of the surface domain is summarized in Table 4.

Table 4. Size of the surface domains used for the MD simulations.

Particle Type	Number of atoms in one layer	Number of layers
Ag309 (silver particle consisting of 309 atoms); Ni309 (nickel particle consisting of 309 atoms)	576 (24×24)	17
Others	144 (12×12)	10

Simulation procedure

The equations of motion were integrated numerically with a typical time step of 2 femtoseconds (fs). The Verlet velocity algorithm (Allen and Tildesley, 1987) was used for the integration. The choice of time step depended on the system studied. The time step is determined to ensure the energy of the system is conserved (the fluctuations of total energy were typically less than 1 ppm).

In the simulation, the particle and surface were first equilibrated independently at a certain temperature (mainly 298 K). After the equilibration, the particle's initial orientation was chosen randomly, and its initial position parallel to the surface was chosen randomly in the unit cell located at the center of the surface. In the vertical direction, particle was initially placed outside the interaction range from surface atoms. The initial velocity of the particle was then assigned. The direction of the initial velocity was normal to the surface. No rotational motion was initially given to the particle. The position and velocity of the atoms of the particle and surface were recorded during the entire simulation period. The obtained data were then analyzed to archive the desired information; e.g., the particle trajectory, the kinetic and potential energies.

For a given particle and surface system, ten microscopically initial states were prepared. At least ten runs were performed for each simulation condition using these states. The bounce probability as the function of simulation parameters was obtained from these multiple runs. The particles were considered to stick to the surface if the particle velocity normal to the surface changed its sign (or direction) twice. The critical velocity (or energy) for particle bounce was defined as the velocity (or energy) for 50% bounce probability.

SIMULATION RESULTS

Collision of Ag particles with an Ag surface

This section presents the simulation results of a particle consisting of 55 silver atoms (Ag55) colliding with a silver surface at 298 K. The Ag55 particle and the surface are shown in Fig. 2 (a). Fig. 3 shows an example of the particle trajectory in the direction perpendicular to the surface. It is for a particle with the initial velocity ($V_{cm,i}$) of 170 m/s and with an energy parameter (ε) of

0.05 eV. Since the z-axis (vertical to the surface) points from the surface to the particle, the particle has a negative velocity initially. Clearly, the particle bounces in this case. The magnitude of the particle final velocity is less than that of initial velocity, indicating that a part of the center-of-mass energy was lost.

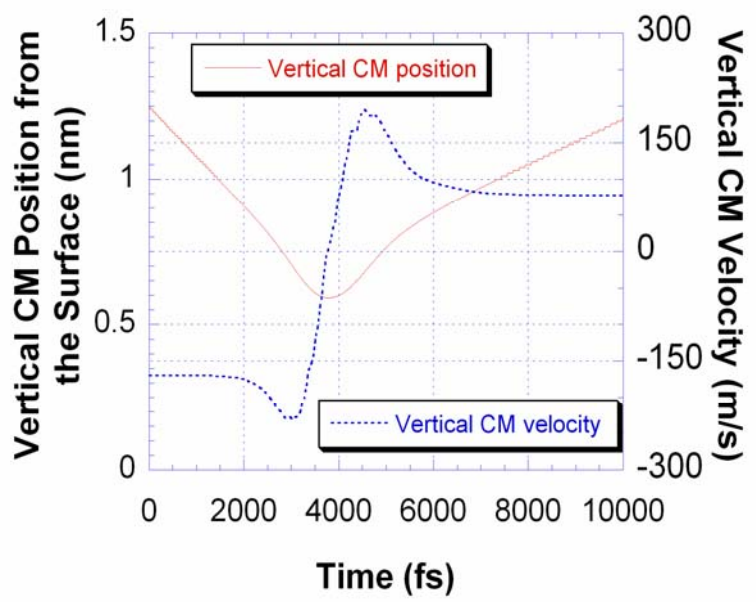

Fig. 3. A trajectory of the Ag55 particle colliding with the silver surface. The left vertical axis shows the center-of-mass (CM) distance from the surface, and the right vertical axis shows the particle CM velocity perpendicular to the surface. The particle initial velocity ($V_{cm,i}$) and the energy parameter (ε) are 170 m/s, and 0.05 eV, respectively.

The bounce probability of Ag55 particle from the silver surface as the function of initial velocity is shown in Fig. 4. For the case of ε = 0.125 eV, the particle sticks to the surface regardless of its initial velocity. For the case of ε = 0.02 eV, there is the velocity below which the particle sticks to the surface. Above the velocity, the bounce probability increases rapidly, reaching unity at approximately $V_{cm,i}$ = 100 m/s. This behavior is similar to that reported for micron-sized particles (e.g., John, 1995). The bounce probability for ε = 0.05 eV shows strange behavior. For initial velocities less than 170 m/s, the bounce probability shows similar behavior as that for ε = 0.02 eV; however, the bounce probability decreases as the initial velocity increases beyond 170 m/s.

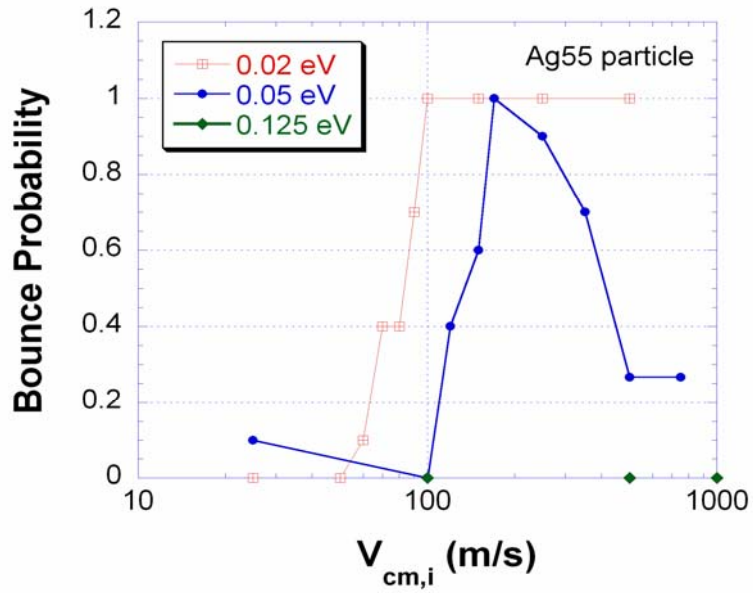

Fig. 4. Bounce probabilities of the Ag55 particle on the silver surface as a function of the initial center-of-mass velocity for ε = 0.02, 0.05, and 0.125 eV.

In order to investigate this strange behavior, the energy changes of the particle and the surface throughout the simulation period were examined. The kinetic and potential energies of the particle for $V_{cm,i}$ = 170 m/s and ε = 0.05 eV as the function of time are shown in Fig. 5 (a). The kinetic energy is divided into four components: the center-of-mass energy (translation energy) in the vertical direction, KE_{cm}; the center-of-mass energy in the horizontal direction, $KE_{cm,h}$; the rotational energy, KE_{rot}; and the random-motion and vibration energy, $KE_{rand,vib}$. $KE_{rand,vib}$ is defined as:

$$KE_{rand,vib} = KE_p - KE_{cm} - KE_{cm,h} - KE_{rot} \quad (6)$$

where KE_p is the total kinetic energy of the particle. As seen in the figure, the center-of-mass energy (in the vertical direction) becomes zero at the elapsed time (t) of about 3700 fs, then goes up and down, and eventually reaches a constant value. The particle potential energy, PE_p, has a temporal increase at t = 3000 - 4500 fs, coinciding with the time of the collision. The potential energy increase is attributed to particle deformation due to the collision. The subsequent decrease indicates that the particle regains its original shape after the collision. Fig. 5 (b) shows the kinetic and potential energies of the surface, KE_s and PE_s. Both energies show a slight increase upon collision. Overall, about 80% of the center-of-mass energy is transferred to other degrees of freedom. The energy loss, however, is not large enough to cause particle deposition onto the surface.

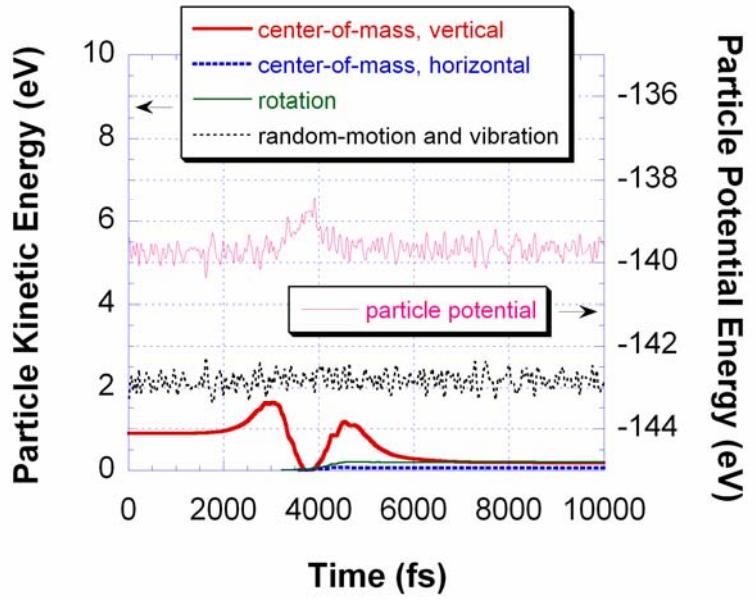

Fig. 5(a). Particle kinetic and potential energies as a function of time during the collision of the Ag55 particle with the silver surface ($V_{cm,i}$ = 170 m/s, ε = 0.05 eV). The kinetic energy is divided into four parts: vertical center-of-mass energy, horizontal center-of-mass energy, rotational energy, and random-motion and vibrational energy.

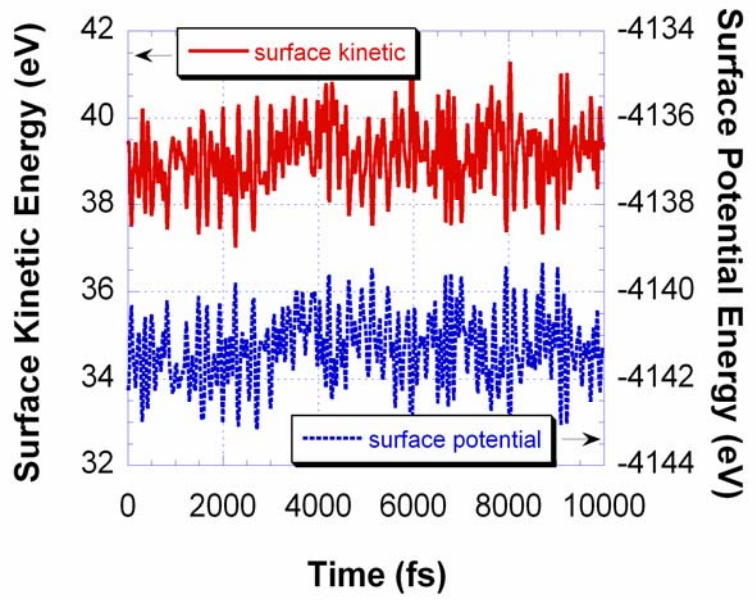

Fig. 5(b). Surface kinetic and potential energies during the collision of the Ag55 particle with the silver surface ($V_{cm,i}$ = 170 m/s, ε = 0.05 eV).

A case for $V_{cm,i}$ = 500 m/s and ε = 0.05 eV is now addressed. The particle and surface energies as the function of elapsed time are shown in Fig. 6 (a) and (b), respectively. In this case, the center-of-mass energy of the particle eventually becomes zero; namely, the particle sticks to the

surface. The distinct difference from the previous case is that the particle potential energy increases by the collision and remains the same afterward. This behavior indicates that the particle deforms permanently. It is also seen that the random-motion and vibration energy increases. Fig. 6(b) also shows that surface vibration is excited due to the collision. It is clear from the results that the decrease in the bounce probability for ε = 0.05 eV is due to energy consumption caused by permanent particle deformation and surface excitation.

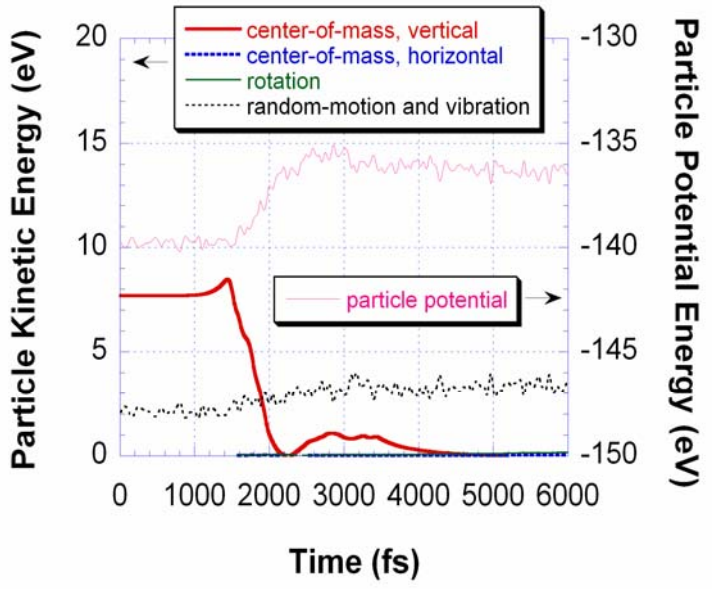

Fig. 6(a). Particle kinetic and potential energies as a function of time during the collision of the Ag55 particle with the silver surface ($V_{cm,i}$ = 500 m/s, ε = 0.05 eV).

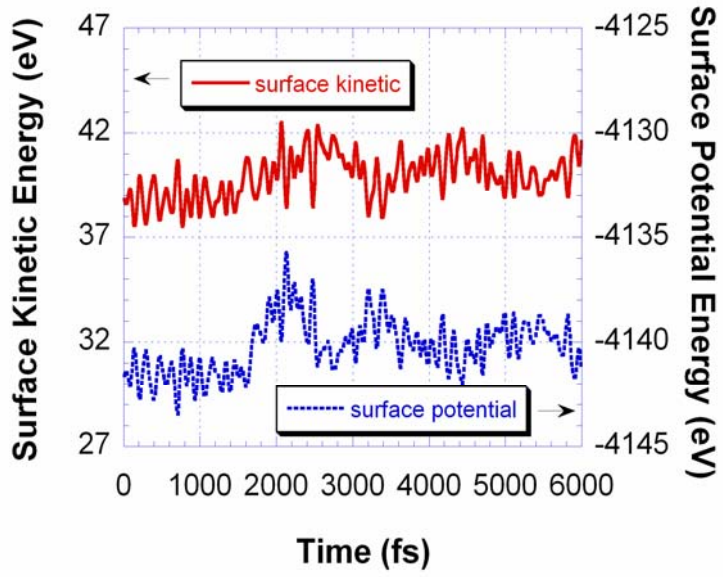

Fig. 6(b). Surface kinetic and potential energies as a function of time during the collision of the Ag55 particle with the silver surface ($V_{cm,i}$ = 500 m/s, ε = 0.05 eV).

Particle size dependence

Simulations of collisions of Ag13 and Ag309 particles with a silver surface were also performed. The bounce probabilities as a function of the initial center-of-mass energy (instead of the velocity) are shown in Fig. 7 (a). The shapes of the bounce probability curves of Ag13 and Ag309 are similar to those of Ag55. The thermal energy in one direction, 1/2kT, is also shown in Fig. 7 (a). The critical energy for particle bounce (initial center-of-mass energy for 50% bounce probability) is much larger than the thermal energy for all of the conditions.

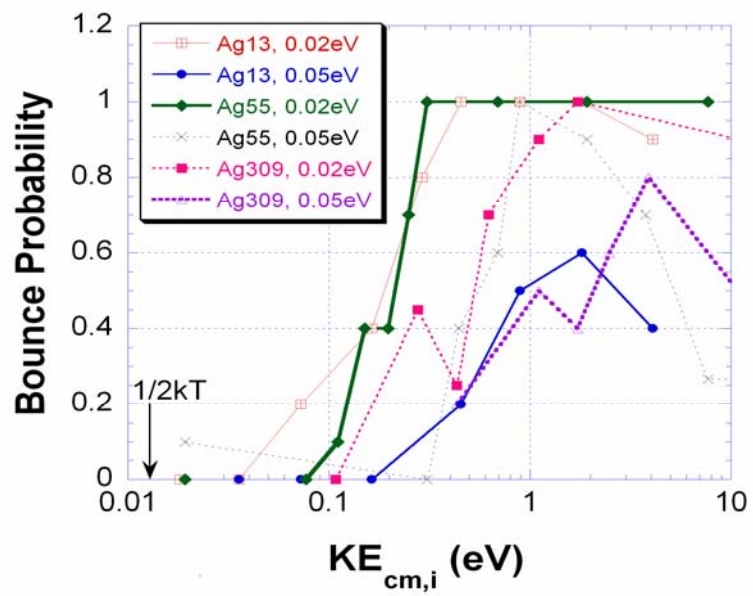

Fig. 7(a). Bounce probabilities as a function of the initial center-of-mass energy, $KE_{cm,i}$, for the Ag13, Ag55, and Ag309 particles colliding with the silver surfaces (ε =0.02, and 0.05 eV). Thermal energy, 1/2kT, at T = 298K is also shown.

Table 5. Adhesion energies, E_{ad}, for all of the particle-surface combinations.

Particle	Surface	ε (eV)	E_{ad} (eV)
Ag13	silver	0.02	0.250
Ag13	silver	0.05	0.761
Ag55	silver	0.02	0.454
Ag55	silver	0.05	1.44
Ag309	silver	0.02	0.931
Ag309	silver	0.05	3.01
Ag13 (500 K)	silver	0.02	0.256
Ag55 (500 K)	silver	0.02	0.479
Ag309 (500 K)	silver	0.02	0.973
Ni13	silver	0.02	0.235
Ni13	silver	0.05	0.758
Ni55	silver	0.02	0.411
Ni55	silver	0.05	1.34
Ni309	silver	0.02	0.784
Ni309	silver	0.05	3.09
Silica54	silver	0.008	0.347
Silica54	silver	0.02	1.20

As can be seen in Fig. 7 (a), the probability curves are spread over a wide energy range. This spread is caused mainly by differences in the adhesion energy. The adhesion energies for all of the particle-surface combinations are listed in Table 5. In general, it is expected that the critical energy for particle bounce increases with the adhesion energy. Therefore, the bounce probabilities may collapse into one curve if they are plotted as a function of the initial center-of-mass energy divided by the adhesion energy ($KE_{cm,i}$ / E_{ad}). The plots are shown in Fig. 7 (b). The probability curves are now much closer to each other as expected. The differences should be attributed to differences in energy losses. In general, the curve shifts to the right (toward a larger $KE_{cm,i}$ / E_{ad}) as energy loss increases. It may be noticed that the curves for the Ag13 particle are positioned to the right of the other curves, suggesting larger energy losses. The experimental bounce probabilities of Ar atoms and NO molecules at a Pt(111) surface are also shown in Fig. 7 (b) (from Kleyn, 1997). The curve for NO is located to the right of that for Ar, which seems reasonable since an NO molecule has more degrees of freedom, to which the translational energy can be transferred. Of particular interest is that the Ag particles do not lose more energy than Ar atoms or NO molecules, despite having more degrees of freedom.

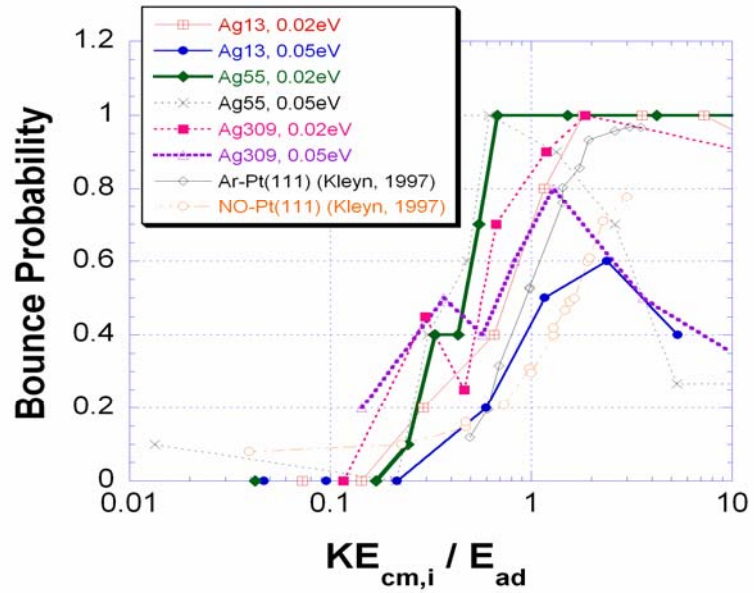

Fig. 7(b). Bounce probabilities as a function of the initial center-of-mass energy divided by the adhesion energy ($KE_{cm,i}$ / E_{ad}) for the silver particles colliding with the silver surfaces (ε = 0.02, and 0.05 eV), along with the results for Ar atoms and NO molecules colliding with a Pt(111) surface (from Kleyn, 1997).

In order to understand the collision dynamics in detail, the energy loss mechanism was investigated. It has been found that a relatively large amount of energy is lost to the horizontal and rotational degrees of freedom, even though the particle does not originally have energies in these degrees of freedom. The energy transfer to the rotational degree is the largest for the largest particles (Ag309). It can account for as much as 60% of the total energy loss. This energy transfer occurs partly because the surface is not completely flat in the atomic scale, and partly because the particles are not completely spherical.

It has also been found the energy loss of the Ag13 particles is mostly due to the energy transfer to the surface, which is not significant for the Ag55 and Ag309 particles. To understand why the Ag13 particles lose more energy to the surface, the energy changes during collision are plotted in Fig. 8 (a) and (b) for the Ag13 and Ag55 particles, respectively. The plots show typical results for each particle size when little permanent deformation of the particle occurs. In the figures, the "particle internal" refers to the particle total energy minus the particle rotational and center-of-mass energies (namely, the sum of the random-motion, vibration, and deformation energy). The "surface" stands for the surface total energy. Except for the vertical center-of-mass energy, the changes from the initial values are shown. As can be seen in Fig. 8 (a), the center-of-mass energy of the Ag13 particle is mainly transferred to the surface as elastic energy upon collision, and that only a small portion of it is recovered when the particle rebounds. The less energy transfer to the particle internal energy is probably due to the fact that the Ag13 particle does not have many

internal degrees of freedoms, compared to the surface or the other particles. In other words, the Ag13 particle behaves like a "spring" with a larger spring constant: the center-of-mass energy is mainly stored as the elastic energy of the surface that has a smaller "spring constant." In the rebound phase, the energy stored in the surface was not completely recovered because of the incompatibility of the "spring constants" (i.e., differences in frequencies of vibration motion). The explanation using the imaginary springs seems justified by the results for the Ag55 particles. As can be seen in Fig. 8 (b), the surface energy and particle internal energy increase by almost the same amount upon collision. Most of these energies are recovered in a similar manner when the particle rebounds. This observation can again be explained using the concept of imaginary springs: the Ag55 particle has enough internal degrees of freedom so that it behaves like a spring whose spring constant is the same as that of the surface.

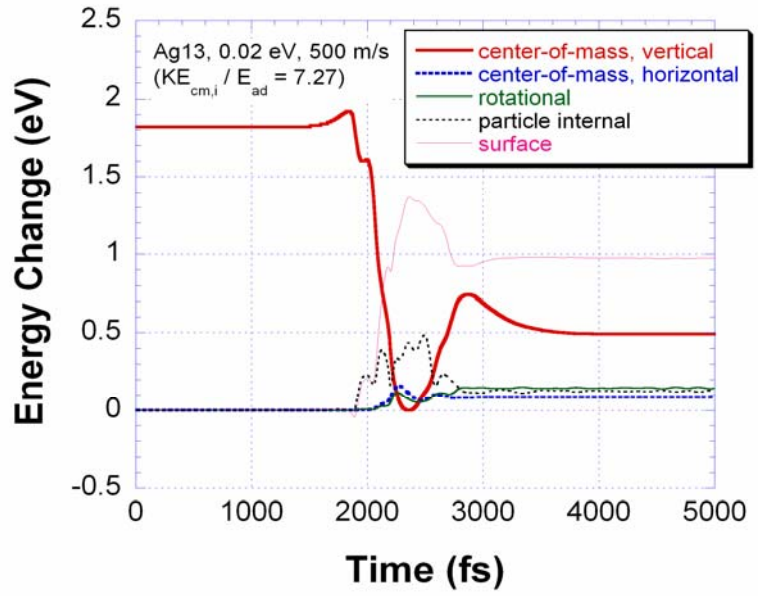

Fig. 8(a). Energy changes during collision. The vertical center-of-mass energy, and the changes of horizontal center-of-mass energy, rotational energy, particle internal energy and surface total energy from the initial values are shown: (a) the Ag13 particle, $V_{cm,i}$ = 500 m/s, ε = 0.02 eV ($KE_{cm,i}$ / E_{ad} = 7.27).

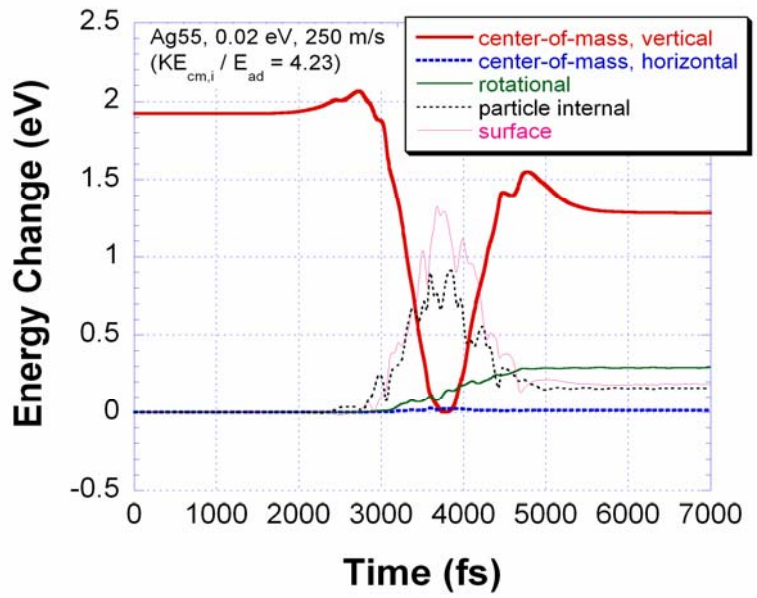

Fig. 8(b). Energy changes during collision. The vertical center-of-mass energy, and the changes of horizontal center-of-mass energy, rotational energy, particle internal energy and surface total energy from the initial values are shown: (b) the Ag55 particle, $V_{cm,i}$ = 250 m/s, ε = 0.02 eV ($KE_{cm,i}$ / E_{ad} = 4.23).

Particle material dependence

(a) Ni particles

If the imaginary spring description proposed in the previous section is valid, particles harder than a surface should lose a relatively larger amount of energy by the collision. In order to test this hypothesis, the collision of nickel particles (Ni13, Ni55, and Ni309) on a silver surface was simulated. The bounce probability as the function of the ratio of initial kinetic energy to the adhesion energy ($KE_{cm,i}$ / E_{ad}) is shown in Fig. 9. All of the probability curves of the Ni particles are positioned to the right of the curve for the Ag55 particle, which indicates more energy losses for the Ni particles.

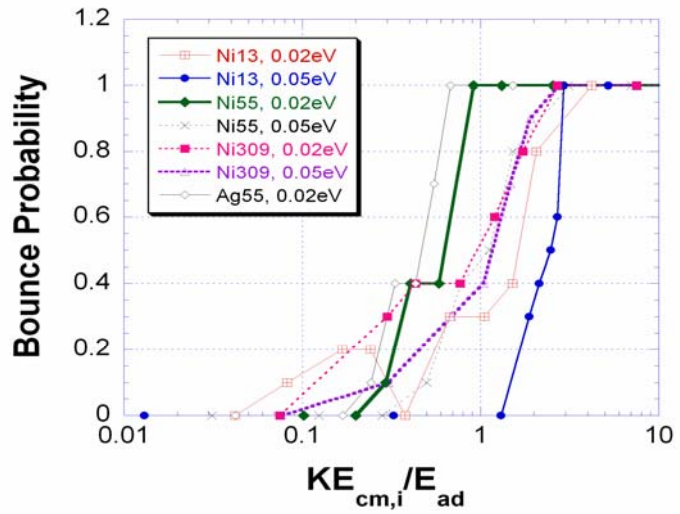

Fig. 9. Bounce probabilities as a function of the initial center-of-mass energy divided by the adhesion energy ($KE_{cm,i}$ / E_{ad}) for the nickel particles colliding with the silver surfaces (ε =0.02, and 0.05 eV), along with the results for the Ag55 particle (ε =0.02 eV).

Energy changes during collision are also given in Fig. 10 (a) and (b) for the Ni13 and Ni309 particles, respectively. Both plots show a similar trend as that of the Ag13 particle. The center-of-mass energy primarily transfers to the surface and only a small fraction is recovered in the rebound phase. Since nickel is harder than silver, this observation can again be explained by the imaginary spring description.

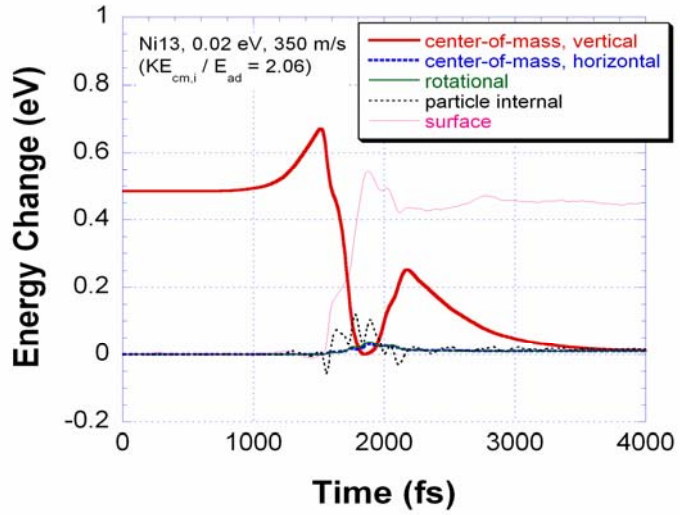

Fig. 10(a). Energy changes during collision. The vertical center-of-mass energy, and the changes of horizontal center-of-mass energy, rotational energy, particle internal energy and surface total energy from the initial values are shown: (a) the Ni13 particle, $V_{cm,i}$ = 350 m/s, ε = 0.02 eV ($KE_{cm,i}$ / E_{ad} = 2.06)

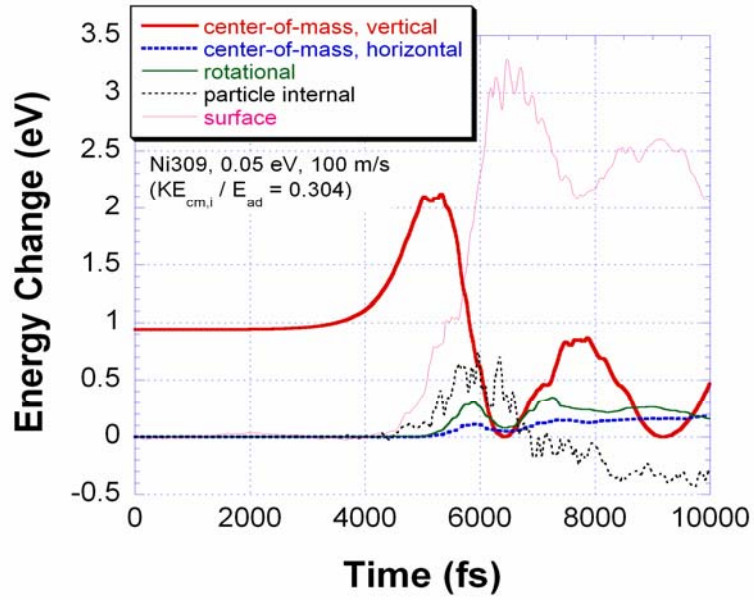

Fig. 10(b). Energy changes during collision. The vertical center-of-mass energy, and the changes of horizontal center-of-mass energy, rotational energy, particle internal energy and surface total energy from the initial values are shown: (b) the Ni309 particle, $V_{cm,i}$ = 100 m/s, ε = 0.05 eV ($KE_{cm,i}$ / E_{ad} = 0.304).

(b) Silica particles

The impaction of a silica particle on an Ag surface was also simulated. The silica particle consisted of 36 oxygen atoms and 18 silicon atoms (Silica54). The particle has a non-spherical shape as shown in Fig. 2 (b). Therefore, the possible effects of a non-spherical shape on the collision dynamics can be investigated in this simulation.

The bounce probabilities of the silica particle for ε = 0.008 eV, and 0.02 eV are shown in Fig. 11. The bounce probability curves are positioned to the far right of that for the Ag55 particle, indicating larger energy losses. On the other hand, it is noteworthy that the bounce probability for ε = 0.008 eV has a relatively long tail at the low-energy side. Fig. 12 (a) and (b) show the energy changes of the silica particle during the collision for two different particle initial velocities. As can be seen in these plots, the rotational excitation upon impact is significant in both the cases. In the case shown in Fig. 12 (a), the particle rotates on the surface and has multiple collisions with the surface. The rotational energy gained by the first collision is transferred to the surface by the multiple collisions in a stepwise manner. Therefore, it can be said that the energy losses to the surface are mediated by particle rotations. This phenomenon is similar to the "rotation mediated adsorption" of a diatomic molecule to a surface (Kuipers *et al.*, 1989a, 1989b). The large energy loss of NO molecules colliding on a Pt(111) surface (see Fig. 7 (b)) could be explained by this phenomenon (Kleyn, 1997). Therefore, particle rotation is actually a key in understanding the large energy loss of the silica particle.

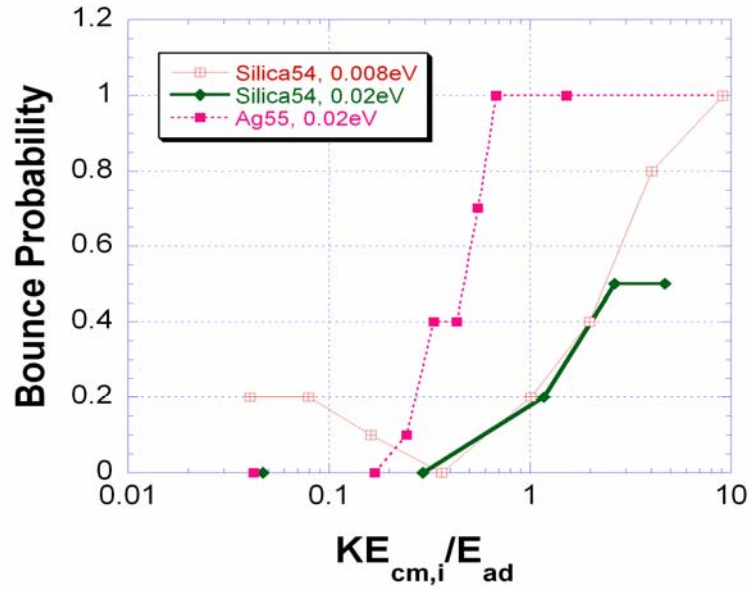

Fig. 11. Bounce probabilities as a function of the initial center-of-mass energy divided by the adhesion energy ($KE_{cm,i}$ / E_{ad}) for the Silica54 particles colliding with the silver surface (ε =0.008, and 0.02 eV), along with the results for the Ag13 particles (ε =0.02 eV).

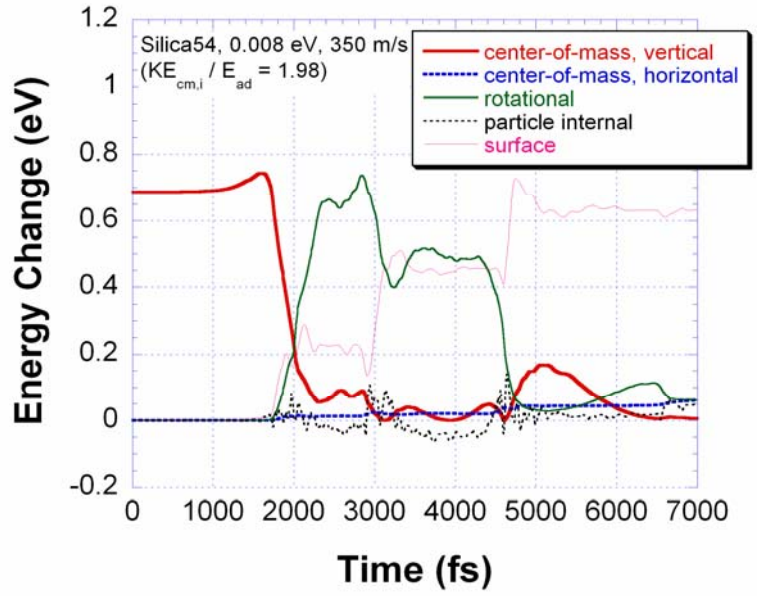

Fig. 12(a). Energy changes during collision. The vertical center-of-mass energy, and the changes of horizontal center-of-mass energy, rotational energy, particle internal energy and surface total energy from the initial values are shown: (a) the Silica54 particle, $V_{cm,i}$ = 350 m/s, ε = 0.008 eV ($KE_{cm,i}$ / E_{ad} = 1.98).

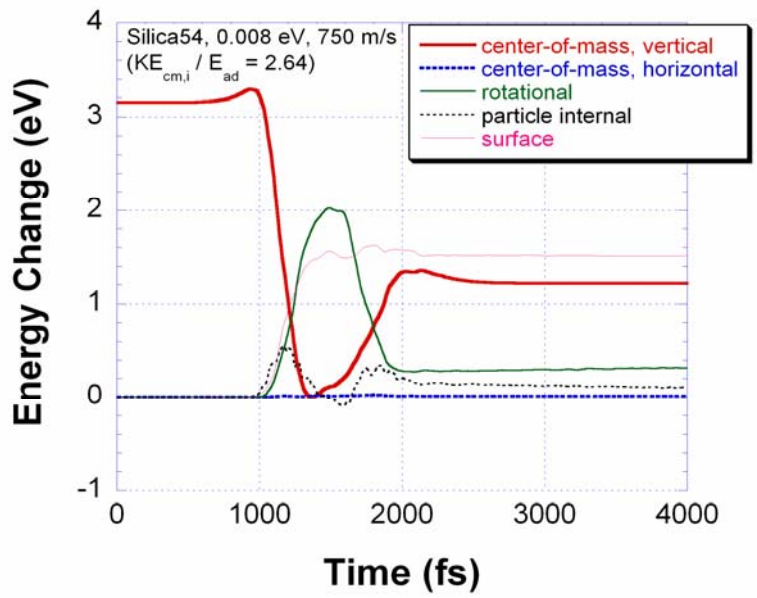

Fig. 12(b). Energy changes during collision. The vertical center-of-mass energy, and the changes of horizontal center-of-mass energy, rotational energy, particle internal energy and surface total energy from the initial values are shown: (b) the Silica54 particle, $V_{cm,i}$ = 750 m/s, ε = 0.008 eV ($KE_{cm,i}$ / E_{ad} = 2.64).

As shown in Fig 12 (b), the rotational energy gained by collision with a surface is occasionally transferred back to the center-of-mass energy. However, this phenomenon is rare, as also implied by Kuipers *et al.* (1989b) for diatomic molecules. Incidentally, Fig. 11 shows that, although the probability is low, the silica particles can bounce at a relatively low $KE_{cm,i}$ / E_{ad}. It was found that this is caused by large variations of the adhesion energy due to their non-spherical shape. Namely, the adhesion energy can be very low, depending on the particle orientation, thus causing occasional particle bounce.

Temperature dependence

The results so far indicate that thermal rebound is unlikely under the simulated conditions (see Fig. 7(a)). However, thermal rebound can happen at higher temperatures if the bounce probability is not affected by the temperature increases. Simulations at a temperature of 500 K were performed to investigate the possible temperature effects. According to Lifshitz (1956), the van der Waals interaction is not affected by temperature if the separation distance is small compared to hc/(2πkT) (h: plank constant; c: speed of light; k: Boltzmann constant; T: absolute temperature). Thus, the interaction potential between the particle and surface atoms was assumed to be unchanged. Fig. 13 shows the bounce probabilities of the Ag55 particles at 500 K, along with the results at 298 K.

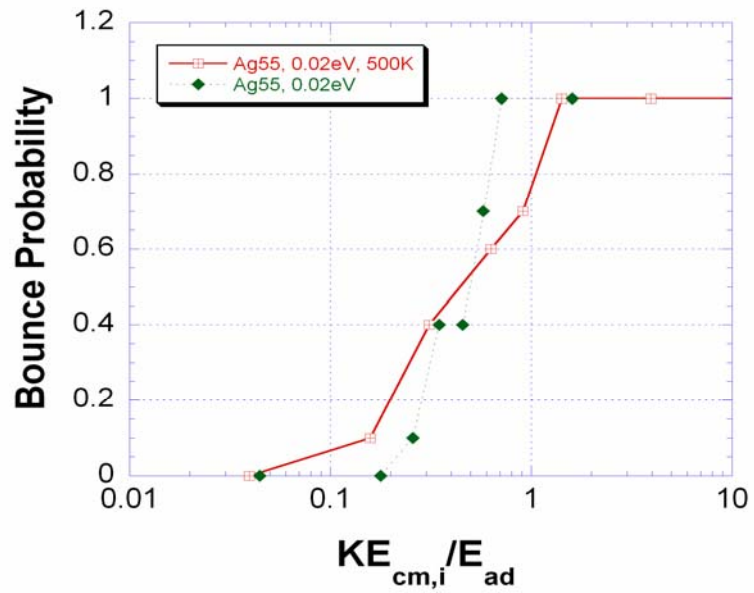

Fig. 13. Bounce probabilities as a function of the initial center-of-mass energy divided by the adhesion energy ($KE_{cm,i}$ / E_{ad}) for the Ag55 particles colliding with the silver surface at T = 500 K (ε =0.02 eV), along with the results at T = 298 K.

The probability curve is less sharp at 500 K. This trend is the same as that for the collision of Ar atoms with a Pt(111) surface (Rettner *et al.*, 1990), which is caused by a broadening of the relative velocity between the particle and the surface due to greater thermal motion of particle and surface atoms. More importantly, the results indicate that the critical energy for particle bounce remains unchanged. This implies that thermal rebound may be possible at a higher temperature. However, this issue is not so straightforward, since the material properties can be different at higher temperatures.

CONCLUSION AND FUTURE WORK

Collision dynamics of nanoparticles with a surface was studied by classical molecular dynamics simulations. Silver was mainly used as particle and surface materials. As for particle materials, nickel and silica were also employed. Approximate particle sizes ranged from 0.5 to 2 nm. The results show that the particles with thermal energy at room temperature do not bounce off a surface, even when a very weak particle-surface interaction potential is assumed. It therefore seems unlikely that thermal rebound can be a serious problem in nanoparticle filtration at room temperature. It should be mentioned that a small fraction of particles with high energy always exist due to the Maxwellian energy distribution, and can therefore bounce off filter surfaces. However, such a fraction is typically less than 0.01% at room temperature under our simulation conditions.

The mechanisms of the center-of-mass energy losses of nanoparticles were also investigated. It was found that energy losses to the surface and the rotational degree of freedom are of great importance. These losses have typically not been considered in studies on micron particle collision with a surface. The loss to the surface is significant when a harder particle hits a softer surface. This is because the center-of-mass energy is mainly transferred to the softer surface as elastic energy, and the energy is not effectively transferred back due to differences in mechanical behavior between the particle and surface. A very small particle, such as the Ag13, also behaves like a harder particle due to small degrees of freedom, and loses more energy to the surface than larger particles. Non-spherical silica particles were found to lose more energy than the other types of particles, due to an effective energy transfer to the rotational degree of freedom. The rotational energy is usually not transferred back to the center-of-mass energy, and is mainly lost to the surface via multiple collisions. By the way, only particles incident perpendicularly to the surface were considered in the simulations. The current results could be applied to particles with different incident angles by considering the normal component of the center-of-mass energy of such particles.

The simulations at a high temperature (500 K) show that the critical energy for particle bounce is unaffected by the temperature increase. This result suggests that thermal rebound might be possible at high temperatures. Moreover, there is the possibility that particles weakly bound to a surface leave it due to thermal fluctuations, like molecules do (Frenkel, 1947; Kuipers *et al.*, 1988). This phenomenon could present a serious problem in nanoparticle filtration, and should be addressed in the future.

ACKNOWLEDGMENTS

We are grateful for the financial support provided by the Minnesota Supercomputing Institute at the University of Minnesota, and the US Department of Energy, Grant No. DOE/DE-FG02-98ER14909.

REFERENCES

Allen, M.P. and Tildesley, D.J. (1987). *Computer Simulation of Liquids*. Clarendon Press, Oxford.

Alonso, M., Kousaka, Y., Hashimoto, T. and Hashimoto, N. (1997). Penetration of Nanometer-sized Particles through Wire screen and Laminar Flow Tube. *Aerosol Sci. Technol*. 27: 471-480.

Andres, R.P. (1995). Inelastic Energy Transfer in Particle/surface Collisions. *Aerosol Sci. Technol*. 23: 40-50.

Bitter, J.G.A. (1963) A Study of Erosion Phenomena. *Wear*, 6: 5-21.

Blömer, J. and Beylich, A.E. (1999). Molecular Dynamics Simulation of Energy Accommodation of Internal and Translational Degrees of Freedom at Gas-surface Interfaces. *Surf. Sci*. 423: 127-133.

Brach, R.M. and Dunn, P.F. (1995). Macrodynamics of Microparticles. *Aerosol Sci. Technol*. 23: 51-71.

Cheng, Y.S. and Yeh, H.C. (1980). Theory of a Screen-type Diffusion Battery. *J. Aerosol Sci*. 11: 313-320.

Cleri, F. and Rosato, V. (1993). Tight-binding Potentials for Transition Metals and Alloys. *Phys. Rev*. B. 48: 22-33.

Dahneke, B. (1972). The Influence of Flattening on the Adhesion of Particles. *J. Colloid Interface Sci*. 40: 1-13.

Dahneke, B. (1973). Measurements of Bouncing of Small Latex Spheres. *J. Colloid Interface Sci*., 45, 584-590.

Dahneke, B. (1975). Further Measurements of the Bouncing of Small Latex Spheres. *J. Colloid Interface Sci*. 51: 58-65.

Donaldson, K., Li X.Y. and MacNee, W. (1998). Ultrafine (Nanometer) Particle Mediated Lung Injury, *J. Aerosol Sci*. 29 (5/6) : 553-560.

Dunn, P.F., Brach, R.M. and Caylor, M.J. (1995). Experiments on the Low-velocity Impact of Microsheres with Planar Surfaces. *Aerosol Sci. Technol*. 23: 80-95.

Frenkel, J. (1946). *Kinetic Theory of Liquids*. Clarendon Press, Oxford.

Gormley, P.G. and Kennedy, M. (1949). Diffusion from a Stream Flowing Through a Cylindrical Tube. *Proc. Roy. Irish Acad*. 52A: 163-169.

Guissani, Y. and Guillot, B. (1996). A numerical Investigation of the Liquid-vapor Coexistence Curve of silica. *J. Chem. Phys*. 104: 7633-7644.

Gupta, R.P. (1981). Lattice Relaxation at a Metal Surface. *Rhys. Rev*. B. 23: 6265-6270.

Huheey, J.E., Keiter, E.A. and Keiter R.L. (1993). *Inorganic Chemistry: Principles of Structure and Reactivity*. 4th Ed. HarperCollins College Publishers, New York.

Hunt, K.H. and Crossley, F.R.E. (1975). Coefficient of Restitution Interpreted as Damping in Vibroimpact. *J. Appl. Mech*. 42: 440-445.

John, W. (1995). Particle-surface Interactions: Charge Transfer, Rnergy Loss, Resuspention, and Deagglomeration. *Aerosol Sci. Technol*. 23: 2-24.

Johnson, K.L., Kendall, K. and Roberts, A.D. (1971). Surface Energy and the Contact of Elastic Solids. *Proc. R. Soc. Lond*. A. 324: 301-313.

Kleyn, A.W. (1997). Non-reactive Orientations of Molecules at Surfaces. *Prog. Surf. Sci*. 54: 407-420.

Kuipers, E.W., Tenner, M.G., Kleyn, A.W. and Stolte, S. (1989a). Steric Effects in Molecular Adsorption due to an Anisotropic Repulsion. *Surf. Sci*. 211/212: 819-828.

Kuipers, E.W., Tenner, M.G., Kleyn, A.W. and Stolte, S. (1989b). Dependence of the NO/Ag(111) Trapping Probability on Molecular Orientaion. *Chem. Phys*. 138: 451-460.

Kuipers, E.W., Tenner, M.G., Spruit, M. E.M. and Kleyn, A.W. (1988). Differential Trapping Probabilities and Desorption of Physisorbed Molecules: Application to NO / Ag(111). *Surf. Sci*. 205: 241-268.

Li, X., Dunn, P.F. and Brach, R.M. (1999). Experimental and Numerical Studies on the Normal Impact of Microspheres with Surfaces. *J. Aerosol Sci*. 30: 439-449.

Lifshitz, E. M., (1956). The Theory of Molecular Attractive Forces between Solids. *Soviet Phys*. 2: 73-83.

Otani, Y., Cho, S.J. and Emi, H. (1994). Romoval of Nanometer Size Particles and Ions from Air. *Proceedings of the 12th ISCC*, Yokohama, Japan, pp. 21-25.

Reed, J. (1989). *The Adhesion of Small Particles to a Surface. In Particles on Surfaces 2: Detection, Adhesion and Removal (Edited by K. L. Mittal)*, pp. 3-17. Plenum, New York.

Rettner, C.T., Mullins, C.B., Bethune, D.S., Auerbach, D.J., Schweizer, E.K. and Weinberg, W.H. (1990). Molecular Beam Studies of Trapping Dynamics. *J. Vac. Sci. Technol*. A. 8: 2699-2704.

Rogers, L.N. and Reed, J. (1984). The Adhesion of Particles Undergoing an Elastic-plastic Impact with a Surface. *J. Phys*. D. 17: 677-689.

Tsai, C.J., Pui, D. Y.H. and Liu, B. Y.H. (1990). Capture and Rebound of Small Particles upon Impact with Solid Surfaces. *Aerosol Sci. Technol*. 12: 497-507.

Tsuneyuki, S., Tsukada, M., Aoki, H. and Matsui, Y. (1988). First-principles Interatomic Potential of Silica Applied to Molecular Dynamics. *Phys. Rev. Lett*. 61: 869-872.

Wall, S., John, W. and Goren, S.L. (1989). *Application of Impact adhesion Theory to Particle Kinetic Energy Loss Measurements. In Particles on Surfaces 2: Detection, Adhesion and Removal (Edited by K. L. Mittal)*, pp. 19-34, Plenum, New York.

Wall, S., John, W., Wang, H.C. and Goren, S. L. (1990). Measurements of Kinetic Energy Loss for Particles Impacting Surfaces. *Aerosol Sci. Technol*. 12: 926-946.

Wang, H.C. and Kasper, G. (1991). Filtration Efficiency of Nanometer-size Aerosol Particles. *J. Aerosol Sci*. 22: 31-41.

Xu, M. and Willeke, K. (1993). Right-angle Impaction and Rebound of Particles. *J. Aerosol Sci*. 24: 19-30.

Received for review, September 21, 2006
Accepted, November 10, 2006